Quantum Dots in Semiconductor Optoelectronic Devices

by Edward B. Stokes, Adrienne D. Stiff-Roberts, and Charles T. Dameron

Nanoscale materials such as semiconductor quantum dots (SQDs) have electronic and optical properties between those of much larger macro and microscale bulk semiconductor crystals, and much smaller atoms and molecules. The investigation of these materials is often envisaged as the cusp of a new field—nanoscience—where heretofore unexplored interactions are possible between practitioners and components of chemistry, physics, biology, and various engineering disciplines.[1]

Because nano-size is of the same order as the Bohr exciton radius of electron-hole pairs in solids, SQDs exhibit quantum size effects, essentially those of quantum mechanical particles in a three-dimensional box.[2] The electronic transition energy from the highest occupied molecular orbital (HOMO) to the lowest unoccupied molecular orbital (LUMO) is a decreasing function of the diameter of the QD, with the limit that the HOMO-LUMO transition energy approaches the semiconductor bandgap as the SQD size approaches of order micron size or larger. The peak wavelength of optical absorption and luminescence emission is determined by the HOMO-LUMO transition energy. SQDs have been produced with peak optical emission wavelengths ranging from the ultraviolet, through the visible, and into the infrared.

SQDs are currently assembled or synthesized using either "dry" or "wet" methods. Dry techniques are the most familiar to the traditional semiconductor microfabrication community, while wet techniques are typically the domain of synthetic chemists. Though submicron nanostructures can also be formed through somewhat traditional paths using a top down approach involving high resolution ultraviolet or electron beam lithography and dry etching (*e.g.*, reactive ion etching), these techniques cannot be used to make true quantum dots of Bohr exciton scale.

True dry Bohr-exciton scale quantum dots are formed using a bottom up approach, with the use of epitaxial techniques to produce SQDs from atomic constituents and/or molecular precursors. Such SQDs are assembled using strained-layer growth in ultra-high vacuum, crystal growth systems, such as molecular beam epitaxy or metal-organic chemical vapor deposition. SQD growth is a consequence of the lattice mismatch between the matrix (or substrate) material and the dot (or epi-layer) material. The minimization of strain energy results in the formation of three-dimensional islands, typically with a pyramidal or lens shape. For most epitaxial QDs, these three-dimensional islands occur during the Stranski-Krastanow (S-K) growth mode, which is characterized by the formation of a two-dimensional, pseudomorphic (or wetting) layer, followed by the three-dimensional QD growth. It is important to note that due to the random nature of this S-K growth mode, fluctuations occur in the size, material composition, and doping of epitaxial QDs. As a result, these materials experience inhomogeneous linewidth broadening (full-width, half-maximum (FWHM) linewidth ~50 meV). This inherent non-uniformity of epitaxial QD ensembles nullifies many of the advantages expected from the zero-dimensional size of a single QD. In the near future, we can expect that, *e.g.*, innovative epitaxial techniques will significantly increase epitaxial SQD uniformity and consequently the performance of SQD optoelectronic devices.

Much recent work is also in the area of bottom up synthesis of wet colloidal SQDs, grown in solution in a chemical reaction vessel. Incorporation of these wet colloidal SQDs into semiconductor devices requires radically different innovations in semiconductor device fabrication technology, because it involves somehow taking the particles out of solution in which they were grown, and placing them as an optically active later in a device heterostructure. Wet SQDs form a major emerging component of the nanomaterial marketplace, and SQDs are commercially available at this writing from a number of small companies, including Evident Technologies in Troy, NY; Crystalplex in Pittsburgh, PA; UT Dots in Urbana-Champaign, IL; NN Labs in Fayetteville, AR; and Q-Dot, recently acquired by biotech giant Invitrogen in Carlsbad, CA. Because SQD particle size, and hence the peak luminescence emission wavelength, can be controlled with great precision in wet colloidal synthesis, and because the surface chemistry of SQDs can be modified to have compatibility with a variety of solvents including water, the first major commercial application of SQD is in luminescent tags for biomedical applications. Wet SQDs can be also assembled into quantum dot solids through various deposition techniques such as drop-casting, spin-casting, and Langmuir-Blodgett methods. Finally, SQDs can in principle be epitaxially overgrown to form device heterostructures with novel nanostructured active layers.

(continued on next page)

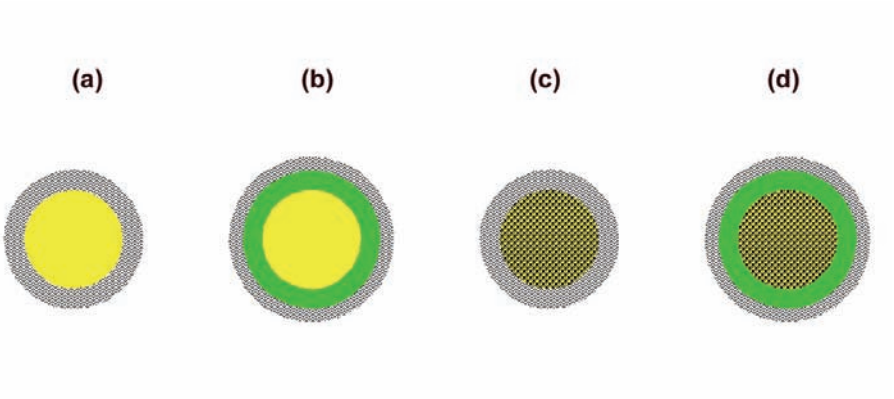

Fig. 1. *Schematic diagrams of simple SQD structures. (a) A CdS SQD core dot (yellow) capped with an organic coat. (b) A core-shell SQD with an organic coated ZnS shell (green) over a CdS core. (c) An alloy SQD with a Cd-Zn-S core capped with an organic coat. (d) An alloy core shell capped SQD. Developed from Bailey and Nye (2003).*

Wet Synthesis of QDs

Synthetic SQDs of a variety of types are readily accessible through colloidal syntheses. Typical syntheses rely on the formation of a nanocrystalline type of core, usually a metal sulfide or selenide such as cadmium sulfide (CdS) or cadmium selenide (CdSe), and then allow for growth under limiting conditions so that small crystallite particles can be formed. Initial cores are formed from metal-organic complexes that serve as nucleation sites for the incorporation of sulfide or selenium. Simplistically, termination of the particle's growth is accomplished through depletion of the ions that are adding to the core of the particle. The growth limitation is accomplished by stopping the further addition of the core ions or by removing the growing dot from the growth medium. Controlling the size of the dots is one method used to make SQDs with specific spectral and chemical properties. In commercial SQDs organic metal ligands such as TOPO or mercapto-acetic acid form a metal-organic complex and nucleation site for sulfide and, subsequently, provide an organic cap on the crystallite to aide in their stability. Nanocrystals are inherently prone to accretion and oxidation. The bulk properties of the SQDs, such as aqueous or hydrocarbon solubility, can be manipulated by modifying the capping molecules. A number of different metal binding organic coats are used by commercial companies depending on the proposed uses of the SQDs.

Properties of the SQDs are further manipulated through the use of hybrid methodologies that produce core shell, alloy, and doped SQDs. A schematic description of commonly accessible colloidal based SQD is shown in Fig. 1. Core shell SQDs are made by applying a secondary layer of another semiconductor which has a greater band gap than the core, for example zinc sulfide (ZnS), over the surface of a CdS or CdSe core. The ZnS layer both increases the intensity of the fluorescence output of the dots and further stabilizes, the dots against accretion and oxidation.[3] Alloy and doped SQDs are cores made with three or more elements such as CdSeS, and in some cases, additional metal ions such as zinc, manganese, or even mercury. Alloys allow a wider range of spectral and chemical properties to be accessed than can be accessed with classical CdS or CdSe QDs, where the spectral properties are directly dependent upon the core size of the SQDs.

Synthetic chemist and Chief Scientific Officer Lianhua Qu, PhD, at Crystalplex, uses secondary metals or metalloids and mixtures of S and Se in the synthesis of alloy SQDs to induce disorder in the crystalline lattice and change the effective mass of the electrons and holes in the SQDs. The changes brought on by the alloy structure are used to tune the spectral features, light absorption and emission, while limiting changes to the particle size.[4] The distinction between an alloy and a doped SQD lies principally in the amount of the additional ions incorporated into the particles. The composition of the alloys does affect the stability of the SQDs, and therefore, their fabrication properties in subsequent processes. The ability to manufacture SQDs with similar sizes but differing spectral properties is a benefit to manufacturing processes that require uniformity such as some types of biological imaging tools. SQDs which have resilient (non-bleaching) fluorescence properties and electron dense cores make them well suited for use as biological labels. In biological applications the SQDs are not subjected to physical extremes in solvents and temperatures. On the other hand, in engineering applications SQDs can often be subjected to high temperatures, extreme pH values, and harsh solvents. The use of alloys can cause unexpected results during device construction. The commercial manufacture of SQDs has been largely directed towards their use in biomedical applications where uniformity in size and surface composition are important but the resistance to physical abuse is less critical for device construction.

To realize their potential in rigorous efficient device manufacture it is essential that the device engineers have a complete understanding of the material composition of the particle core and coat of the SQD. The type and surface density of the metal binding organic molecules on the surface, for instance, changes the manner in which the SQDs behave in manufacturing processes. It is clear that the chemical properties of the metal-binding ligands that form the SQD cap have profound effects on the solubility of the SQDs in solutions. Indeed, some manufacturers sell aqueous and non-aqueous (hydrocarbon) soluble SQDs. It is also clear that in physical device manufacture the capped SQDs interact to form organized non-random structures when dried onto surfaces (e.g., gallium nitride) or embedded in matrices (e.g., silicon). Changes in the capping process, the surfaces or matrices, or the solvents used change the resultant secondary structures and therefore, ultimately, the spectral properties of the devices.[5-8]

Incorporating QDs into Detector Devices

Motivation for using semiconductor QDs in photodetectors.—Compared to higher-dimensional quantum well and bulk active regions, QDs are advantageous for photodetection due to the effects of three-dimensional quantum confinement. Perhaps the most important advantage is the broad spectral range available (UV to the far-IR) by controlling tuning parameters, such as shape, size, strain, and material composition. Through the careful control of carrier occupation, QDs are also eligible to participate in interband and/or intraband transitions, further extending the spectral response capability of a given QD system. Importantly, normal-incidence detection is permitted for QD transitions according to polarization selection rules, thereby overcoming a significant limitation in quantum well photodetectors. In addition, large, excited-state electron relaxation times (resulting from the phonon bottleneck) contribute to increased detector efficiency because photogenerated carriers are more likely to be collected. It is important to note that one of the most important characteristics of a QD ensemble is uniformity. The ensemble absorption coefficient is inversely proportional to its linewidth, thus, a more uniform QD ensemble will experience a greater absorption coefficient, leading to enhanced detector efficiency.

Classes of semiconductor QDs for photodetectors: epitaxial quantum dots.—Epitaxial QDs are embedded in a wider-bandgap matrix material by epitaxial overgrowth. Depending on the band-lineup of the QD and matrix materials, QD confinement barriers are created in the conduction and/or valence bands, thereby providing an additional mechanism for quantum confinement. These confinement barriers are important in that, when combined with selective carrier occupation through doping, the independent control of electron and/or hole populations is enabled, and excitonic phenomena need not be considered. Because higher-dimensional active regions do not experience momentum conservation for transitions within a single band, intraband transitions have been investigated almost exclusively for photodetector applications using epitaxial QDs. Typically, the energy levels are closely spaced such that intraband transitions are in the infrared range, and quantum dot infrared photodetectors (QDIPs) have been studied extensively as a result.

Common QDIP material systems include III-V compound semiconductors (especially InAs/GaAs) and Group IV semiconductors

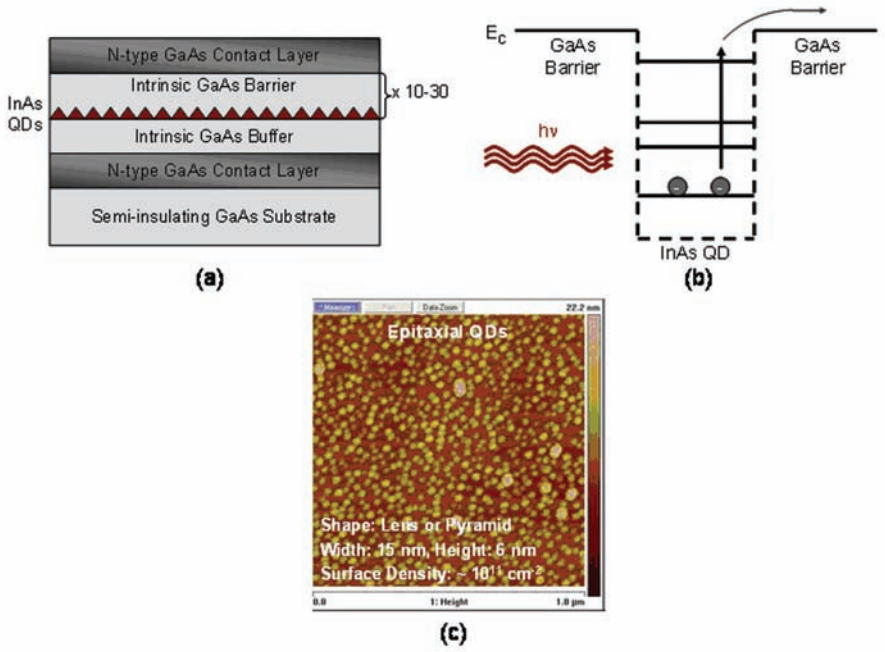

Fig. 2. *Schematic diagrams of (a) device heterostructure and (b) energy vs. position of intraband transitions demonstrating photocurrent generation in epitaxial, InAs/GaAs quantum dot infrared photodetectors. (c) Atomic force microscopy image of epitaxial InAs/GaAs QDs demonstrating important structural characteristics.*

(especially Ge/Si) (see Fig. 2). QDIPs typically contain 10-30 QD layers separated by large barrier regions to prevent the propagation of strain through the heterostructure. Two-terminal devices with a lateral or vertical configuration are fabricated, and these devices typically have two n-type contacts to collect electrons. The most important advantage of QDIPs is the promise of high-operating temperature (≥150 K) due to reduced dark current as a result of three-dimensional carrier confinement. Low dark current,[9-11] multi-spectral response,[12-14] high-detectivity,[15] high-temperature photodetection,[16,17] and IR imaging[18,19] have been demonstrated in QDIPs. Thus, these devices should enable high-performance IR camera systems with reduced cost, size, and weight.

Classes of semiconductor QDs for photodetectors: colloidal QDs.— Colloidal QDs could improve photodetector performance compared to epitaxial QDs due to *(i)* control over colloidal QD synthesis and ability to conduct size-filtering, leading to highly-uniform ensembles; *(ii)* spherical shape of colloidal QDs, simplifying calculations for device modeling and design; and *(iii)* greater selection of active region materials since strain considerations that dominate the growth of epitaxial QDs are eliminated. Typically, colloidal QDs are applied to optoelectronic devices as conducting polymer/nanocrystal blends, or nanocomposites, as in solar cells.[20-22] Colloidal QD solids have also been investigated.[23] The application of colloidal QDs to photodetector applications is a relatively new endeavor, and is still largely focused on the detection of IR light,[24-28] thus photodetector nanocomposites often feature narrow-bandgap, II-VI, colloidal QDs, such as PbSe or PbS (see Fig. 3).

It is important to note that colloidal QD nanocomposites exhibit subtle differences compared to epitaxial QDs. First, intraband transitions are not exploited. Instead, interband transitions of excitons across the polymer and colloidal QD bandgaps contribute to the photoresponse of the detector. Second, the polymer acts as the active region, and the colloidal QDs enhance photocurrent at specific wavelengths corresponding to their size. This enhancement occurs since colloidal QDs are electron acceptors and the polymer is a hole conductor such that excitons are dissociated at their interface. Thus, photoconduction through the nanocomposite occurs as electrons hop among QDs and holes transport through the polymer. Colloidal QD photodetectors typically comprise a single nanocomposite layer deposited on a glass slide by spin-casting, and large-area, two-terminal, vertical devices are fabricated using p- (indium-tin-oxide) and n-type (aluminum) contacts. An important future direction is to develop hybrid devices featuring epitaxial and colloidal QDs in a single device heterostructure to enable unprecedented flexibility in the spectral response of photodetectors.[29-31]

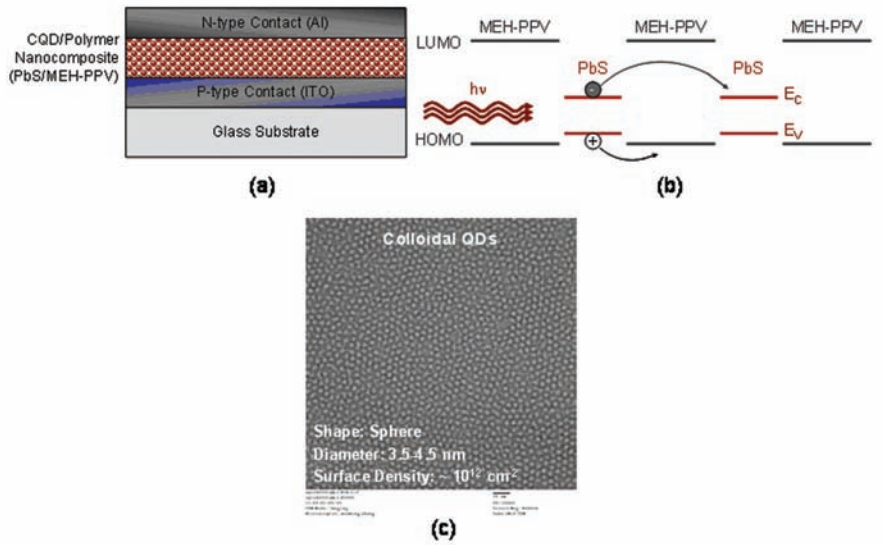

Fig. 3*. Schematic diagrams of (a) device heterostructure and (b) energy vs. position of interband transitions demonstrating photocurrent generation in colloidal PbS QD/ MEH-PPV conducting polymer nanocomposites for infrared photodetection. (c) Transmission electron microscopy image of colloidal CdSe/CdS core-shell QDs demonstrating important structural characteristics, such as increased uniformity across the ensemble.*

Quantum Dots and Nanostructure in Light Emitting Diodes

A typical InGaN-GaN light emitting diode (LED) heterostructure is shown in Fig. 4b. Under forward bias, electrons and holes from the n-type and p-type clad recombine in the active InGaN layer to produce photons in the blue to green spectral region. Initial speculation on the viability of such III-nitride based microelectronics was pessimistic even after p-doping challenges were solved by Akasaki, et al.[32,33] Large area native III-nitride substrates for strain free epitaxial growth of III-nitride materials are an area of current development and a promising emerging technology,[34] but are not yet widely used due to

(continued on next page)

perceived price and/or availability. So, most GaN-InGaN heterostructures are grown on sapphire or silicon carbide. The former has a 16% lattice mismatch to GaN, while the latter has a better 3.4% lattice mismatch,[35] but a potentially crack-inducing tensile thermal expansion mismatch when epitaxial films are cooled from typical metal-organic chemical vapor deposition (MOCVD) growth temperatures of 1100-1200C.[36] Largely because of poor substrate compatibility, typical MOCVD grown GaN-InGaN heterostructure materials have threading dislocation densities of order $10^9/cm^2$, a factor of 10^6 or so higher than historically required for good functionality of GaAs family LEDs (e.g. Fig. 4a). So, by traditional logic, InGaN-GaN heterostructure LEDs should not function, since the delocalized electron and hole wavefunctions in an InGaN quantum well should significantly interact with the threading dislocations, which themselves are non-radiative[37] or suboptimal[38,39] recombination centers. However such LEDs do function quite well, with wall plug efficiencies in excess of 20% for the best currently commercially available devices. It turns out that nanostructure plays a critical role in the high performance of these recently ubiquitous blue and green LED devices.

When InGaN quantum well active layers are grown by MOCVD, high indium fraction compositional inhomogeneities, with relatively low bandgap, naturally form on the nanoscale, acting to confine electron hole pairs and isolate them from the surrounding low indium fraction, wider bandgap material in the quantum well.[40] There is active debate as to whether these high indium fraction regions should be called quantum dots or simply compositional inhomogeneities. In any case, electron-hole pairs that fall into these high indium fraction regions do not interact with the threading dislocations, and tend to recombine radiatively, resulting in high efficiency devices. But this high efficiency only is achievable with InGaN over a limited wavelength range; for wavelengths shorter than about 400 nm, the indium fraction is too low, and for wavelengths longer than about 550 nm, the compositional inhomogenieties are extended beyond the nanoscale. In any case, the nanoscale high indium fraction regions partly enable the high performance in the blue and near-green spectral regions.

So how can SQD be used to develop optoelectronic materials with wavelengths between GaAs and GaN? Assembly of colloidal SQDs into larger mesostructures, and integration with semiconductor devices, is the subject of a great deal of current research and development. Drop-cast and spin-cast CdSe quantum dot solids have been formed on, e.g., glass substrates, their electronic and optical properties have been characterized, and some progress has been made on assembling them into photodetectors.[41] Fluorescence and atomic force micrographs of drop cast CdSe SQD mesostructures on MOCVD GaN are shown in Fig. 5. To overcome the efficiency limitations of InGaN LEDs in the deep green spectral region (550-590 nm), CdSe-ZnS core-shell quantum dots have been employed as the active layer in both organic LEDs[42] and in various inorganic device structures. CdSe quantum dots on a surface have been demonstrated to be pumped on the surface of an InGaN LED heterostructure through a non-radiative energy transfer mechanism.[43] Since the melting point of SQD is suppressed relative to bulk semiconductor materials, in inorganic LEDs with colloidal SQD active layers (*e.g.*, Fig. 4c), care must be taken to epitaxially overgrow the SQDs without destroying them. In one recent study, CdSe-ZnS SQDs were deposited on MOCVD p-GaN and a novel low temperature n-GaN layer was deposited using the ENABLE technique.[44] In other recent work, CdSe-ZnS SQDs were spin-cast on MOCVD n-GaN and overgrown with MBE p-GaN.[45] In both of these inorganic examples, electrically pumped luminescence of encapsulated SQDs has been demonstrated, though at wall plug efficiency less than 0.1%. Electroluminescence from a yellow CdSe SQD LED in a GaN matrix is shown in Fig. 6.

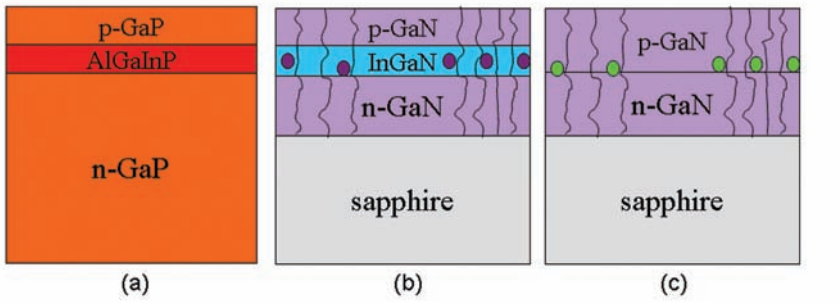

Fig. 4. *Evolution of quantum dot light emitting diodes (LEDs). In all cases, the light emitting diode heterostructure consists of n-type, active, and p-type layers grown epitaxially on a substrate. (a) In the traditional red GaAs family light emitting diode, the epitaxial layers are grown on a lattice matched GaAs substrate, so that the crystal defect density is low. This is a true quantum well LED. (b) In the more recent blue and near-green GaN family LEDs, the epitaxial layers are typically grown on a poorly lattice matched substrate such as sapphire, so that crystal defect densities are high. But high indium fraction quantum dots form in the active layer during epitaxial growth. These QDs serve as radiative recombination centers and keep the electron-hole pairs away from the defects during device operation, resulting in high efficiency. (c) To move device operation outside the range of capability of InGaN, into the deep green for example, several groups are epitaxially overgrowing CdSe quantum dots that are deposited from solution through drop casting or spin casting, for example.*

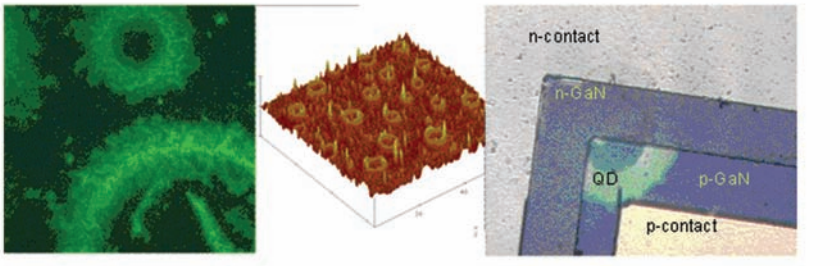

Fig. 5. *Drop-cast CdSe-ZnS core-shell quantum dots on MOCVD n-GaN, overgrown with MBE p-GaN. Evaporation of solvent drives SQD assembly into quantum dot solid micro rings about 20 micrometers in diameter. Left: fluorescence micrograph; center: atomic force micrograph; right: SQD quantum dot solid micro ring incorporated into active mesa of GaN heterostructure LED.*

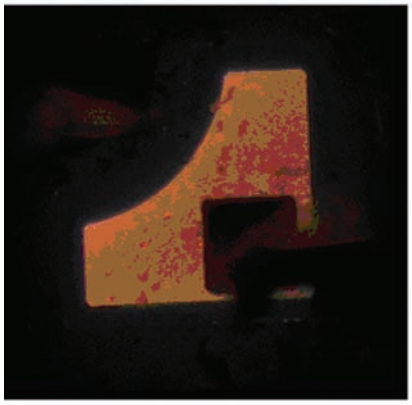

Fig. 6. *Electroluminescence from a GaN heterostructure LED with CdSe-ZnS core-shell quantum dot active layer.*

Conclusion

In the future, we can expect many new products and processes based on nanostructured materials and semiconductor quantum dots. Nanostructure currently plays a key role in the high efficiency performance of III-nitride heterostructure LEDs. As assembly, synthesis, and deposition techniques improve, both wet and dry semiconductor quantum dots will be effectively incorporated into optoelectronic devices to improve performance and enable higher efficiency photodetectors and emitters. ■

Acknowledgments

E. B. S. acknowledges support from the Defense Advanced Research Projects Agency, the Department of Energy, Dot Metrics Technologies, and the National Science Foundation.

A. D. S.-R. acknowledges support from the National Science Foundation, the Air Force Office of Scientific Research, and UNC Charlotte Center for Optoelectronics and Optical Communications.

C.T.D. acknowledges support from Duquesne University, the National Institutes of Health, and Crystalplex Corp.

References

1. L. Venema, *Nature*, **442**, 994 (2006).
2. L. Brus, *IEEE J. Quantum Electron.*, **22**, 1909 (1986).
3. R. E. Bailey and S. Nie, *J. Am. Chem. Soc.*, **125,** 7100-6 (2003).
4. R. E. Bailey and S. Nie, *J. Am. Chem. Soc.*, **125**, 7100 (2003).
5. D. J. Milliron, S. M. Hughes, Y. Cui, L. Manna, J. Li, L-W. Wang, and A. P. Alivisatos, *Nature*, **430**, 190 (2004).
6. E. Rabani, D. R. Reichman, P. L. Geissler, and L. E. Brus, *Nature,* **426**, 271 (2003).
7. M. Z. Rong, M. Q. Zhang, H. C. Liang, and H. M. Zeng, *Appl. Surf. Sci.*, **228**, 176 (2004).
8. R. Xu and H. C. Zeng, *Langmuir,* **20**, 9780 (2004).
9. S. Y. Wang, S. D. Lin, H. W. Wu, and C. P. Lee, *Appl. Phys. Lett.*, **78**, 1023 (2001).
10. A. D. Stiff-Roberts, X. H. Su, S. Chakrabarti, and P. Bhattacharya, *IEEE Photonics Tech. Lett.*, **16**, 867 (2004).
11. X. H. Su, S. Chakrabarti, P. Bhattacharya, G. Ariyawansa, and A. G. U. Perera, *IEEE J. Quantum Electron.*, **41**, 974 (2005).
12. S. Krishna, S. Raghavan, G. von Winckel, P. Rotella, A. Stintz, C. P. Morath, D. Le, and S. W. Kennerly, *Appl. Phys. Lett.*, **82**, 2574 (2003).
13. U. Sakoglu, S. Tyo, M. M. Hayat, S. Raghavan, and S. Krishna, *J. Opt. Soc. Am. B*, **21**, 7 (2004).
14. S. Chakrabarti, X. H. Su, P. Bhattacharya, G. Ariyawansa, and A. G. U. Perera, *IEEE Photonics Tech. Lett.*, **17**, 178 (2005).
15. J. Jiang, S. Tsao, T. O'Sullivan, W. Zhang, H. Lim, T. Sills, K. Mi, M. Razeghi, G. J. Brown, and M. Z. Tidrow, *Appl. Phys. Lett.*, **84**, 2166 (2004).
16. J.-W. Kim, J.-E. Oh, S.-C. Hong, C.-H. Park, and T.-K. Yoo, *IEEE Electron Device Lett.*, **21**, 329 (2000).
17. S. Chakrabarti, A. D. Stiff-Roberts, P. Bhattacharya, S. Gunapala, S. Bandara, S. B. Rafol, and S. W. Kennerly, *IEEE Photonics Tech. Lett.*, **16**, 1361 (2004).
18. A. D. Stiff-Roberts, S. Chakrabarti, S. Pradhan, B. Kochman, and P. Bhattacharya, *Appl. Phys. Lett.*, **80**, 3265 (2002).
19. J. Jiang, K. Mi, S. Tsao, W. Zhang, H. Lim, T. O'Sullivan, T. Sills, M. Razeghi, G. J. Brown, and M. Z. Tidrow, *Appl. Phys. Lett.*, **84**, 2232 (2004).
20. N. C. Greenham, X. Peng, and A. P. Alivisatos, *Synth. Met.*, **84**, 545 (1997).
21. D. S. Ginger and N. C. Greenham, *Phys. Rev. B*, **59**, 10622 (1999).
22. R. Plass, S. Pelet, J. Krueger, M. Grätzel, and U. Bach, *J. Phys. Chem. B*, **106**, 7578 (2002).
23. C. A. Leatherdale, C. R. Kagan, N. Y. Morgan, S. A. Empedocles, M. A. Kastner, and M. G. Bawendi, *Phys. Rev. B*, **62**, 2669 (2000).
24. S. A. McDonald, P. W. Cyr, L. Levina, and E. H. Sargent, *Appl. Phys. Lett.*, **85**, 2089 (2004).
25. K. R. Choudhury, Y. Sahoo, T. Y. Ohulchanskyy, and P. N. Prasad, *Appl. Phys. Lett.*, **87**, 073110 (2005).
26. D. C. Oertel, M. G. Bawendi, A. C. Arango, and V. Bulovic, *Appl. Phys. Lett.*, **87**, 213505 (2005).
27. D. Qi, M. Fischbein, M. Drndic, and S. S elmic, *Appl. Phys. Lett.*, **86**, 093103 (2005).
28. G. Konstantatos, I. Howard, A. Fischer, S. Hoogland, J. Clifford, E. Klem, L. Levina, and E. H. Sargent, *Nature*, **442**, 180 (20 06).
29. M. C. Hanna, O. I. Mii, M. J. Seong, S. P. Ahrenkiel, J. M. Nedeljkovi, and A. J. Nozik, *Appl. Phys. Lett.*, **84**, 780 (2004).
30. A. Madhukar, S. Lu, A. Konkar, Y. Zhang, M. Ho, S. M. Hughes, and A. P. Alivisatos, *Nano Lett.*, **5**, 479 (2005).
31. A. D. Stiff-Roberts, A. Gupta, *et al.*, Materials Research Society Spring Meeting (2006).
32. H. Amano, M. Kitoh, K. Hiramatsu, and I. Akasaki, *J. Electrochem. Soc.*, **137**, 1639 (1990).
33. W. Gotz, N. M. Johnson, J. Walker, D. P. Bour, H. Amano, and I. Akasaki, *Appl. Phys. Lett.*, **67**, 2666 (1995).
34. L. J. Schowalter, S. B. Schujman, W. Liu, M. Goorsky, M. C. Wood, J. Grandusky, and F. Shahedipour-Sandvik, *Phys. Status Solidi A*, **203**, 1667 (2006).
35. M. Leszczynski, *Appl. Phys. Lett.*, **69**, 73 (1996).
36. K. Wang and R. R. Reeber, *MRS Internet J. Nitride Semicond. Res.*, 4S1, G3.18 (1999).
37. T. Sugahara, M.Hao, T. Wang, D. Nakagawa, Y. Naoi, K. Nishino, and S. Sakai, *Jpn. J. Appl. Phys.*, **37**, L1195 (1998).
38. X. H. Wu, C. R. Elsass, A. Abare, M. Mack, S. Keller, P. M. Petroff, S. P. DenBaars, and J. S. Speck, *Appl. Phys. Lett.*, **72**, 692 (1998).
39. O. Martinez, J. Jiminez, M. Bosi, M. Albrecht, R. Fornari, R. Cusco, and L. Artus, *Mat. Sci. Semicond. Proc.*, **9**, 2 (2006).
40. V. Kachkanov, K. P. O'Donnell, R. W. Martin, J. F. W. Mosselmans, and S. Pereira, *Appl. Phys. Lett.*, **89**, 101908 (2006).
41. D. C. Oertel, M. G. Bawendi, A. C. Arango, and V. Bulovic, *Appl. Phys. Lett.*, **87**, 213505 (2005).
42. S. Coe, W. K. Woo, M. Bawendi, and V. Bulovic, *Nature*, **420**, 808 (2002).
43. M. Achermann, M. A. Petruska, D. D. Koleske, M. H. Crawford, and V. I. Klimov, *Nano Lett.*, **6**, 1396 (2006).
44. A. H. Mueller, M. A. Petruska, M. Achermann, D. J. Werder, E. A. Akhadov, D. D. Koleske, M. A. Hoffbauer, and V. I. Klimov, *Nano Lett.*, **5**, 1039 (2006).
45. J. G. Pagan, E. B. Stokes, K. Patel, C. C. Burkhart, M. T. Ahrens, P. T. Barletta, and M. O'Steen, *Solid-State Electron.*, **50**, 1461 (2006).

About the Authors

Edward Stokes is an associate professor of electrical and computer engineering at the University of North Carolina at Charlotte. His current research is focused on development of nanoscale active layer materials for semiconductor optoelectronic devices. He is a member-at-large of the ECS Electronics and Photonics Division executive committee and may be reached at ebstokes@uncc.edu.

Adrienne D. Stiff-Roberts studied applied physics at the University of Michigan, Ann Arbor, and received her doctoral degree under the supervision of Pallab Bhattacharya in Ann Arbor in 2004. In August 2004, she joined Duke University as an assistant professor in the department of Electrical and Computer Engineering. Her current scientific interests range from the epitaxial growth and characterization of quantum-confined semiconductor materials; to the synthesis and characterization of hybrid organic/inorganic nanomaterial thin films; to the design, fabrication, and characterization of optoelectronic and photonic devices, especially in the infrared regime. She is a member of the Institute of Electrical and Electronics Engineers and the Materials Research Society. She is also involved in the program committees for the 2006 North American Conference on Molecular Beam Epitaxy (NA-MBE) and 2007 Conference on Lasers and Electro-Optics (CLEO). She may be reached at adrienne.stiffroberts@duke.edu.

Charles T. Dameron is an associate professor of chemistry and biochemistry at Duquesne University, Pittsburgh. His research focus is on the use of metal ions to stabilize molecular interactions between proteins and other complex molecules. He can be reached at dameron@duq.edu.